Send Orders for Reprints to reprints@benthamscience.net

Current Nanoscience, **2014,** *10,* **695-699**

Novel Iron-oxide Catalyzed CNT Formation on Semiconductor Silicon Nanowire

Tijjani Adam* and U. Hashim

Institute of Nano Electronic Engineering (INEE), Universiti Malaysia Perlis (UniMAP), 01000 Kangar, Perlis, Malaysia

Abstract: An aqueous ferric nitrate nonahydrate ($Fe(NO_3)_3.9H_2O$) and magnesium oxide (MgO) were mixed and deposited on silicon nanowires (SiNWs), the carbon nanotubes (CNTs) formed by the concentration of Fe_3O_4/MgO catalysts with the mole ratio set at 0.15:9.85 and 600°C had diameter between 15.23 to 90nm with high-density distribution of CNT while those with the mole ratio set at 0.45:9.55 and 730°C had diameter of 100 to 230nm. The UV/Vis/NIR and FT-IR spectroscopes clearly confirmed the presence of the silicon-CNTs hybrid structure. UV/Vis/NIR, FT-IR spectra and FE-SEM images confirmed the silicon-CNT structure exists with diameters ranging between 15-230nm. Thus, the study demonstrated cost effective method of silicon-CNT composite nanowire formation *via* Iron-oxide Catalyze synthesis.

Keywords: High-density, hybrid structure, iron-oxide catalyze, SiNWs, silicon-CNT structure.

INTRODUCTION

CNT composites have important role in different fields of nanotechnology, their optical, electrical, thermal and mechanical properties have been widely found to be promising in many applications [1, 2]. There are numerous approaches to use CNTs properties to synthesize new nanodevices ranging from various CNT-metals composites, CNT-ceramics composites and CNT-polymers composites using different techniques. In this study, we intended to improve, SiNWs electrical performance by treating them with CNT coated composites [2, 3] because silica coated CNTs have been proved to be super-dielectric with a very large low-frequency dielectric coefficient and low dielectric loss. In order to improve the sensitivity of bio-molecule detection, the outer surface of the oxide layer of silicon nanowires (SiNWs) is generally equipped with a functional bio-interface consisting of receptor molecules [4-6]. This bio-interface plays a key role in the detection of target bio-molecules. The working principle is as follows: When a target molecule comes in close contact with the receptor, there appear non-negligible partial charges in the combination of receptor and target molecules. This modulates the surface charge profile of the functional layer. Modification in the surface charge, in turn, affects distribution of electrostatic potential throughout the nanowire [7-9]. This change in electrostatic potential affects the conductance of the nanowire which can be detected as fluctuations in current when a voltage is applied at the appropriate terminals of the silicon nanowire [2, 10-12]. However, due to the high resistance of nanowire, it behaves almost like an insulator which makes it less sensitive. To overcome this problem, surface engineering is required, and for the purpose of surface engineering to improve electrical properties, CNT is the best candidate. Thus, there are numerous literatures which discussed that when silicon nanowire is coated with CNT, its properties such as strength, electrical conductivity, and optical properties can be improved and enhanced to serve as stable detection platform [16-20].

A number of researchers have worked on this and as a result, a reasonable number of research articles on the topic appear in the literature. Among them, [1, 2] considered a formation of CNT on functionalized graphene film grown by chemical vapor deposition [1-3, 14]. They introduced an active terminal group containing SAM onto CVD graphene film which could be useful to uniformly bind CNTs onto the film surface and to encourage the fabrication of other nanomaterials. On the other hand, they coated silica molecules with multi-wall carbon nanotubes (MWCNTs) using a sol-gel method and found out that MWCNTs coated uniformly with silica molecules, act as the template to synthesize silica-NTs [18, 19]. Among others, different methods such as liquid phase deposition and plasma- enhanced chemical vapor deposition with various catalytic recipes such as nickel, C_{60} etc. have been successfully used [1-4, 14]. In spite of these efforts, a simple, cheap and commercially deployable solution is yet to be achieved.

MATERIALS AND METHOD

The work starts with the preparation of networks of four nanowires formed using photolithography coupled with oxidation based trimming process, followed by conventional impregnation method applied to prepare the catalysts because the type of the catalyst is important for the growth and morphology of the CNTs. Cobalt, iron, titanium, nickel, copper, zeolites, C_{60} and combinations of these metals and/or their oxides are widely used catalyst materials. In

*Address correspondence to this author at the Institute of Nano Electronic Engineering (INEE), Universiti Malaysia Perlis (UniMAP), 01000 Kangar, Perlis, Malaysia; Tel/Fax: + 60 11125 15077;
E-mail: tijjaniadam@yahoo.com

1875-6786/14 $58.00+.00

this study, metal catalyst of Fe was impregnated in MgO substrate. Iron nitrate ($Fe(NO_3)_3.9H_2O$) was separately mixed with magnesium (MgO) substrate in ethanol solution by ultrasonic mixer with Fe and MgO mole ratio set at 0.15:9.85 and 0.45:9.55 according to the procedure of (Liu *et al*., 2011) [15]. The amount of nitrate in the solution of nitrate, MgO and ethanol was calculated according to the molecular ratios of metals in the compound. The solution of $Fe(NO_3)_3.9H_2O$, MgO and ethanol was mixed for 60 minutes in "Bandelin Sonopuls" ultrasonic mixer and was then kept in oven at 90°C for 24 hours. The dried catalyst-substrate mixture was then ground to avoid any agglomeration that may affect the interaction between acetylene gas and the surface of mixture. The stainless steel reactor was then mounted in an electrical furnace and heated in N_2 flow (99.999% purity, supplied by SittTatt Industrial Gases Sdn. Bhd.) with a flow rate of 40ml/min. Then, high purity methane (99.999% purity, supplied by Malaysian Oxygen Bhd.) mixed with nitrogen with 1:1 (v/v) was passed through the quartz tube once the temperature was stable. The reaction lasted for 30 min, after that the furnace was switched off and the nitrogen was kept flow at 40ml/min until temperature was 100°C. The CNTs in black powder form were finally collected from the quartz reactor for characterization. The characterization of CNT production generally requires the presence of a metal catalyst. The selection of a proper metallic catalyst and process temperature may affect the morphology amount of the synthesized product or the diameter distribution, in this study the effects of temperature and ratio of different catalysts (iron three) to the substrate (magnesium-oxide) on production of CNTS in decomposition of methane were identified using different characterization techniques. The structures of formed CNTs were investigated by field emission scanning electron microscopy (FESEM), AFM, UV/Vis and FTIR.

RESULTS AND DISCUSSIONS

Prior to the coating process of the CNT, the nanowire was fabricated using standard CMOS photolithography, the AFM image can be seen from Fig. (**1a**) and the CNT coated device is shown in Fig. (**1b**). From Fig. (**2**), we can see that radial breathing mode (RBM) corresponds to both radial and lateral presence of the carbon nanotube and its frequency ν_{RBM} (in cm^{-1}) is shifted and depends on the carbon nanotube diameter d as, $\nu_{RBM}= G/d + G'$ (where G and G' are variables dependent on the environment in which the nanotube is present and planar vibrations. For silicon nanowire approximately in range of 10nm, radial breathing mode frequency ν_{RBM} can be estimated as $\nu_{RBM} = 234/d + 10$ for SWNT which is very useful in understanding the CNT diameter from the RBM position.

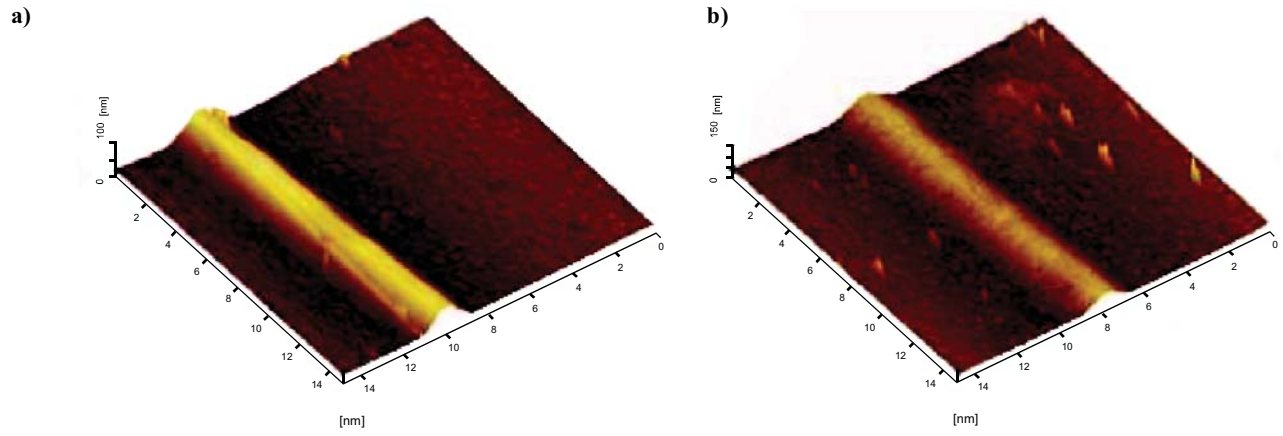

Fig. (1). (**a**) The AFM images of the 5nm Si nanowires before coating process, while (**b**) The AFM images 7nm Si-CNT after coating process.

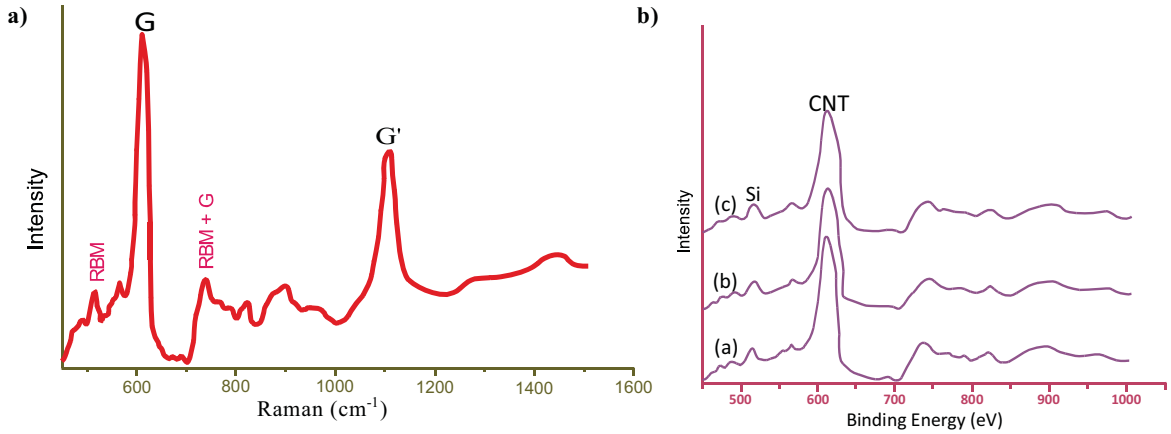

Fig. (2). (**a**) Raman spectrum of single-wall carbon nanotubes present on the surface of the silicon nanowire and (**b**) showing the Raman spectra of three strong peaks in the spectrum of Silicon, CNT and Oxide.

From Fig. (**2a**), it can be seen that typical RBM range is 100–450 $cm^{-1}$and RBM intensity is weak and a bit strong intensity at RBM +G second overtone can be observed at double Raman shift. In Fig. (**2b**), the Raman spectra of three strong peaks in the spectrum for binding energy indicating silicon, CNTs, and oxide are presented where there curves are indicated as a, b, and c, which are showing silicon CNTs at three different intensities with corresponding binding energies. The peaks at ≈500 and 650eV are assigned to the induced phonon and G-line tangential modes in silicon respectively. A photon with a wavelength of ≈500 nm would have an energy of approximately 1-1.33 eV. Similarly, a photon with wavelength >650 and <700 would have an energy of approximately 4-5.1 eV. In turn this electro volt corresponds to band gap of silicon and carbon allotrope such as diamond and approximately close graphene.

The FESEM monograph image shown in Fig. (**3a**) clearly indicates that CNTs are present with a wall thickness ranging between 15 to 30nm. From the FESEM monograph image shown in Fig. (**3b**) revealing the result of the etched CNT on the silicon nanowire, it is clearly confirmed that CNTs have covered the whole nanowire dimension to form silicon-CNTs composite wire with a diameter of silicon-CNTs ranging between 15 to 50 nm.

Fig. (**4**). shows the observed intensity spectrum of Raman shift spectra of the three products of elements present oxide, silicon and silicon-CNTs composite. The saturated normalized spectral intensity of intermediate SiO_2 has a clear peak at around 869cm^{-1}. The intensity of the silicon has decreased at most of the spectral region because the intermediate oxide vicinal surface suppressed due to the abrupt compositional transition. However, the target product, which is the silicon-CNTs composite has shown a very high intensity in the entire spectrum, compared with silicon oxide and silicon. It is quite clear that the optical properties of Silicon-CNTs have brought new phases of material. The results observed from UV/Vis/NIR spectra of the deposited samples indicate that silicon-CNTs dominated device active area, raman spectra of the deposited samples of silicon-CNTs are shown in Fig. (**2**). For silicon the strong intensity corresponds to 550 (eV) bind-

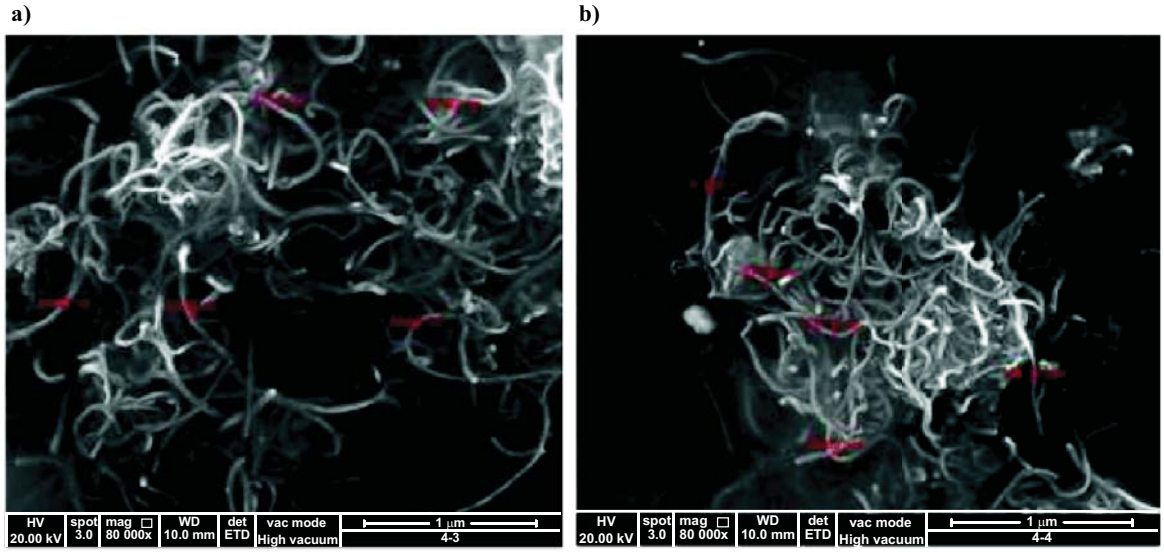

Fig. (3). The FESEM monograph image (**a**) CNT coated device prior etching and (**b**) After Ar and O_2 plasma etching.

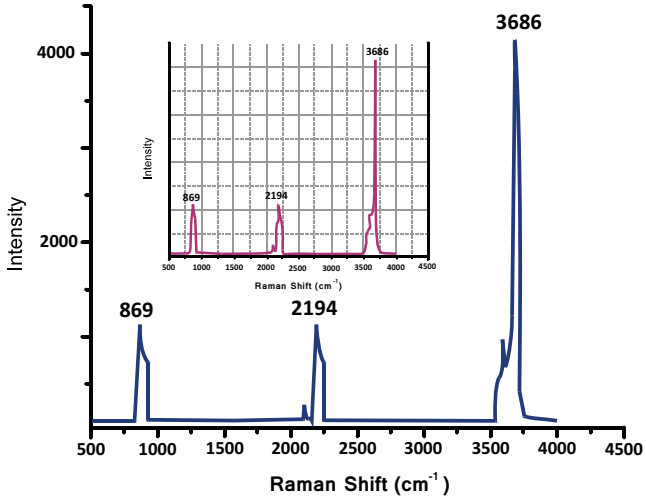

Fig. (4). The Raman shift of the three elements phases including oxide phase, silicon phase and silica-CNTs phase.

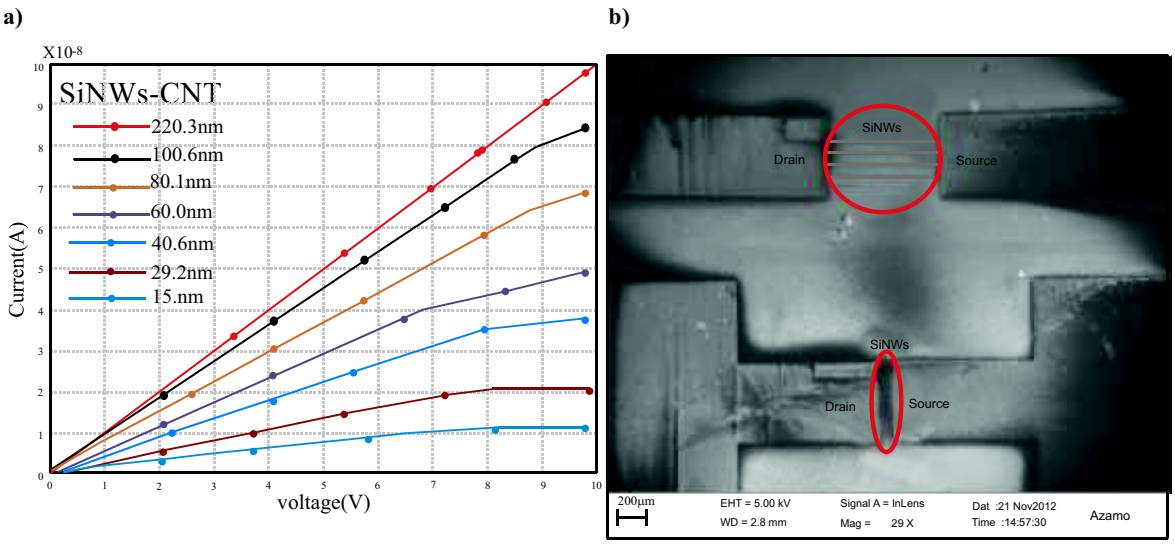

Fig. (5). (**a**) Current-voltage (I-V) (**b**) Network of 4 wire with gold electrode.

ing energy corresponding to Si-O-Si compositional transition due to symmetric stretching vibration. However, in Fig. (**4**), two peaks observed at 869 and 2194 cm^{-1} are attributed to Si-O-Si asymmetric stretching vibration and Si-O shear stretching [1-3]. The Silicon-CNT stretching vibration is observed at 3686 cm^{-1}. On the other hand, in Fig. (**3b**) two peaks with binding energy at 550 and 750 (eV) are observed, which are attributed to the shear stretching and binding energy due to compositional transition of oxide vicinal face for Si-O-Si respectively.

In Fig. (**5**), Keithley 4200 Semiconductor Parameter Analyzer (SPA) method is used to monitor the variation of the resistance of silicon nanowire over 10V. The conductance is characterized by observing current-voltage (I-V) curve which is obtained in the voltage ranging from 1V to 10V. During the measurement set-up, a typical resistor setting is employed on to the two terminal NW devices by supplying voltages to the source (S) region and the output current at the drain (D) region is obtained as shown in Fig. (**5b**). For this experiment, devices with different widths (W) of wires approximately (W = 15nm, 29.2nm, 40.6nm, 60.0nm, 80.1nm, 100.6nm, and 220.3nm,) are characterized. CNTs modified silicon nanowire has a drastically reduced band gap which is confirmed by its optical spectra as shown in Fig. (**4**). Since high intensity of a photon is absorbed by an atom exciting and conductivity depends on both carrier concentration and mobility [13], there are a variety of possible dependencies for conductivity on band gap as can be seen in Fig. (**5a**).

CONCLUSIONS

The study demonstrated the development of a simple yet cost effective method of silicon-CNT composite nanowire formation *via* Iron-oxide Catalyze synthesis. The silicon-CNT composites were produced. The results of UV/Vis/NIR and FT-IR spectroscopes clearly confirm the presence of the silicon-CNTs hybrid structure. The FESEM monograph images also indicate that silicon-CNT is coated and trimmed *via* Ar- O_2 plasmas shallow anisotropic etching. Both UV/Vis/NIR, FT-IR spectra and FESEM images confirm that silicon-CNT structure exists with diameters ranging between 15-230nm.

CONFLICT OF INTEREST

The authors confirm that the article content has no conflict of interest.

ACKNOWLEDGEMENTS

The authors wish to thank Universiti Malaysia Perlis (UniMAP and Ministry of Education Malaysia for giving FRGS grant to conduct this research in the Micro & Nano Fabrication Lab. Appreciation also goes to all the team members in the Institute of Nanoelectronic Engineering especially the Nano structure Lab On chip Research Group.

REFERENCES

[1] Anantram, M.P.; L´eonard F. Physics of carbon nanotube electronic devices. *Rep. Prog. Phys.*, **2006**, *69*, 507-561.

[2] Bandaru, P.R. Electrical Properties and Applications of Carbon Nanotube Structures. *J. Nanosci. Nanotechnol.*, **2007**, *7*, 1-29.

[3] Adhikari, P.D.; Jeon, S.; Cha, M.-J.; Jung, D.S.; Kim, Y.; Park, C.-Y. Immobilization of carbon nanotubes on functionalized graphene film grown by chemical vapor deposition and characterization of the hybrid material. *Sci. Technol. Adv. Mater.*, **2014**, *15*, 1-8.

[4] Hashim, U.; Shahrul A.B.A.; Adam, T. Fabrication of Polysilicon Nanowires using Trimming Technique. *J. Appl. Sci. Res.*, **2012**, *8*(4), 2175-2186.

[5] Chee, P.S.; Arsat, R.; Adam, T.; Hashim, U.; Abdul Rahim, R.; Leow, P.L. Modular architecture of non-contact pinch actuation micropump. *Sensors, **2012**, 12*(9), 12572-12587.

[6] Adam, T.; Hashim, U.; Sutikno; Dhahi, Th.S.; Nazwa, T. Material Engineering for Nano Structure Formation: Fabrication and characterization. Elsevier Procedia Engineering, **2012**, *50*, 361-368

[7] Tsai, S.-P.; Ma, Y.-F.; Sung, M.-J.; Huang, D.-W. Nanofluidic Refractive-Index Sensors Formed by Nanocavity Resonators in Metals without Plasmons. *Sensors,* **2011**, *11*, 2939-2945.

[8] Lin, Y.-S.; Yang, C.-S.; Wang, C.-Y.; Chang, F.R.; Huang, K.-S.; Hsieh, W.-C. An Aluminum Microfluidic Chip Fabrication Using a Convenient Micromilling Process for Fluorescent Poly(DL-lactide-*co*-glycolide) Microparticle Generation. *Sensors,* **2012**, *12*, 1455-1467.

[9] Doria, G.; Conde, J.; Veigas, B.; Giestas, L.; Almeida, C.; Assunção, M.; Rosa, J.; Baptista, P.V. Noble Metal Nanoparticles for Biosensing Applications. *Sensors,* **2012**, *12*, 1657-1687.

[10] Song, K.-M.; Lee, S.; Ban, C. Aptamers and Their Biological Applications. *Sensors,* **2012**, *12*, 612-631.

[11] Suzuki, Y. Exploring Transduction Mechanisms of Protein Transduction Domains (PTDs) in Living Cells Utilizing Single-Quantum Dot Tracking (SQT) Technology. *Sensors*, **2012**, *12*, 549-572.

[12] Jen, C.-P.; Hsiao, J.-H.; Maslov, N.A. Single-Cell Chemical Lysis on Microfluidic Chips with Arrays of Microwells. *Sensors,* **2012**, *12*, 347-358.

[13] Shimosako, Y.; Numai, T. Analysis of Light Intensity Characteristics in Semiconductor Ring Lasers. *Jpn. J. Appl. Phys.*, **2002**, *41*, 1400-1408.

[14] Malekfar, R.; Rajabi, M.H.; MajlessAra, M.H. Structural and Optical Characteristics of Silica Nano-tubes Using CNTs as Template. *Nano-Micro Lett.*, **2010**, *2*(4), 268-271.

[15] Liu, W.-W.; Aziz, A.; Chai, S.-P.; Mohamed, A.R.; Tye, C.-T. Preparation of iron oxide nanoparticles supported on magnesium oxide for producing high-quality single-walled carbon nanotubes. *New Carbon Mater.*, **2011**, *26*(4), 255-261.

[16] Lee, S.-F.; Chang, Y.P.; Lee, L.-Y. Synthesis of carbon nanotubes on silicon nanowires by thermal chemical vapor deposition. *New Carbon Mater.*, **2011**, *26*(6), 401-407.

[17] Afanasov, I.M.; Lebedev, O.I.; Kolozhvary, B.A.; Smirnov, A.V.; Van Tendeloo, G. Nickel/Carbon composite materials based on expanded Graphite. *New Carbon Mater.*, **2011**, *26*(5), 335-340.

[18] Leong, T.G.; Lester, P.A.; Koh, T.L.; Call, E.K.; Gracias, D.H. Surface Tension-Driven Self-Folding Polyhedra. *Langmuir*, **2007**, *23*(17), 8747-8751.

[19] Li, L.-l.; Pan, L.-j.; Li, D.-w.; Zhao, Q.; Ma H. Field emission properties of carbon nanocoils synthesized on stainless steel. *New Carbon Mater.*, **2014**, *29*(1), 34-40.

[20] Laheaar, A.; Delpeux-Ouldriane, S.; Lust, E.; Beguin, F. Ammonia Treatment of Activated Carbon Powders for Super capacitor Electrode Application. *J. Electrochem. Soc.*, **2014**, *161*(4), A568-A575.

Received: March 19, 2014 **Revised: June 02, 2014** **Accepted: June 24, 2014**